ORIGINAL PAPER

Effect of Welding Parameters on Tensile Properties and Fatigue Behavior of Friction Stir Welded 2014-T6 Aluminum Alloy

**Hakan Aydin · Mümin Tutar · Ali Durmuş ·
Ali Bayram · Tayfun Sayaca**

Abstract The present work describes the effect of welding parameters on the tensile properties and fatigue behaviour of 2014-T6 aluminum alloy joints produced by friction stir welding (FSW). Characterization of the samples has been carried out by means of microstructure, microhardness, tensile properties and fatigue behaviors. The hardness in the softened weld region decreases with decreasing the welding speed. Irrespective of the tool rotation speeds, the best tensile and fatigue properties were obtained in the joints with the welding speed of 80 mm/ min. The joint welded with a rotating speed of 1520 rpm at 80 mm/min has given a highest tensile and fatigue properties. The fatigue behaviors of the joints are almost consistent with the tensile properties, especially elongations. Higher ductility in FSW joints made the material less sensitive to fatigue. The location of tensile fractures of the joints is dependent on the welding parameters. On the other hand, the fatigue fracture locations change depending on the welding parameters and stress range. In addition, a considerable correlation could not be established in between heat indexes and mechanical properties of FSW 2014-T6 joints under the investigated welding parameters.

Keywords Friction stir welding · 2014 aluminum alloy · Microhardness · Tensile properties · Fatigue behaviour

H. Aydin (✉) · M. Tutar · A. Durmuş · A. Bayram
Faculty of Engineering and Architecture,
Department of Mechanical Engineering, Uludağ University,
16059 Görükle-Bursa, Turkey
e-mail: hakanay@uludag.edu.tr

T. Sayaca
TDM Automotive Industry Trade Limited Company,
Bursa, Turkey

1 Introduction

Friction stir welding (FSW) is a solid-state joining process invented by TWI in 1991 that is presently attracting considerable interest and has been extensively developed for aluminum alloys, as well as for magnesium, copper, titanium and steel [1–5]. FSW has a wide application potential in ship building, aerospace, automobile, railway and other manufacturing industries [6]. However, the FSW process requires a complete and deep understanding of the technological process and the achieved mechanical behavior, in order to be considered for large scale production of industrial components [7]. FSW offers several advantages over conventional fusion welding processes, due to its low heat input and absence of melting and solidification process [3, 5]. Compared to conventional fusion welding methods, the advantages of the FSW process include better mechanical properties, low residual stress and distortion, and reduced occurrence of defects [1, 4]. This is due to the solid-state joining and a weld zone with fine worked or recrystallized grain structure generated by stirring and forging during FSW [8, 9]. The most important benefits of FSW are its ability to weld the materials that were thought of difficult to be welded, such as aluminum alloys of 2xxx and 7xxx series [3, 5].

The FSW joint is created by friction heating with simultaneous severe plastic deformation of the weld zone material [10]. In this process a cylindrical tool is rotated and traversed along a square butt weld joint similar to milling technique [5]. The joined material is plasticized by heat generated by friction between the surface of the plates and the contact surface of a special tool, composed of two main parts: shoulder and pin [9, 11]. The noticeable microstructure changes in the weld zone for FSW aluminum alloys are divided in: Nugget zone (NZ) in the centre

of the weld where the pin has passed; Thermo-mechanically affected zones (TMAZ) that are immediately on each side of the nugget; Heat affected zones (HAZ) adjacent to the TMAZ that experiences a thermal cycle but does not undergo any plastic deformation, and the unaffected base metal (BM) [12–14]. This complicated microstructure around the weld zone strongly governs the mechanical properties of FSW joints [15, 16].

Fatigue is one of the main causes of failure of welded structures, therefore many efforts have been done to investigate the fatigue properties of FSW aluminum alloy joints [10, 15–20]. However, up to now the material property data, especially for fatigue, for the FSW joints of 2014-T6 aluminum alloys, which is difficult to be joined by conventional fusion welding techniques, was relatively deficient. According to our knowledge, no published results have been presented on the fatigue behaviors of FS welded 2014-T6 aluminum alloys with particular attention to the variation of welding parameters. The welding parameters are the key art of FSW process [5]. The main parameters which characterize the FSW process are the rotation speed and the welding speed. To produce the best weld quality, these parameters have to be determined for each new component and alloy. In this experimental study, the hardness profiles, tensile properties and fatigue behavior of 2014–T6 aluminum plates, friction stir welded at different welding and rotating speeds, were investigated to examine the effect of the welding parameters on the mechanical properties and the fatigue behavior of FSW 2014-T6 aluminum alloys.

2 Experimental Procedure

The material to be welded in the experiments was a 2014 commercial aluminum alloy in the T6-temper state under the form of rolled plates of 3 mm thickness, whose chemical composition (wt%) are listed in Table 1. 2014 aluminum plates were friction stir welded longitudinally parallel to the rolling direction in the butt configuration using a vertical milling machine. The welding procedure can be seen schematically in Fig. 1. The welding parameters used in this investigation are listed in Table 2. A non-consumable tool made of 1.2367 (X38CrMoV5-3) hardened steel with a flat shoulder of 17 mm in diameter was used for all welds. A threaded cylindrical pin used for the

welds has a length 2.9 mm along with a left-hand screw of 0.8 mm pitch and a conical shape with a large diameter of 5 mm and small diameter of 4 mm. The tilt degree of stir pin relative to the work-piece was set equal to 2.5° during welding process. The penetration depth was adapted to fully penetrated butt joint in a material of 3 mm thickness. For all joints a 30 s preheat time was applied in order to increase the plasticity of the material and decrease the bending loads on the pin.

After welding, the joints were cross-sectioned perpendicular to the welding direction for microstructural examination, micro-hardness measurement, tensile and fatigue tests. Prior to that, 45 mm at the beginning and 25 mm at the end of the plate were removed to exclude possible deviation from steady state during start and stop. Microstructures of various zones of the welds resulting from the FSW process are analyzed by means of optical microscopy and micro-hardness measurements. The specimens for the microstructural analyses of the cross-sections were prepared according to standard metallographic practice. The mechanically polished surfaces were chemically etched with Keller's reagent (5 ml nitric acid, 2 ml hydrofluoric acid, 3 ml hydrochloric acid, and 190 ml distilled water) in order to enable the identification of the different weld
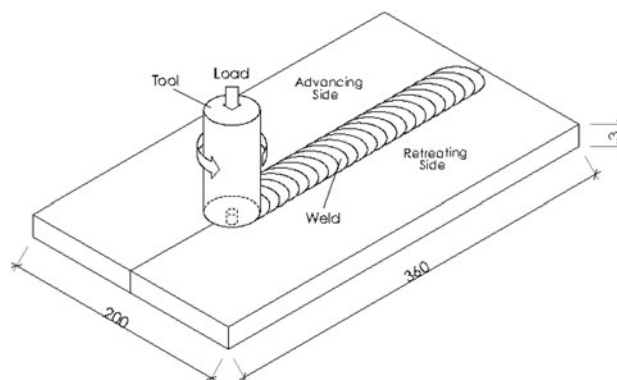

Fig. 1 Schematic illustration and geometrical configuration of FSW process
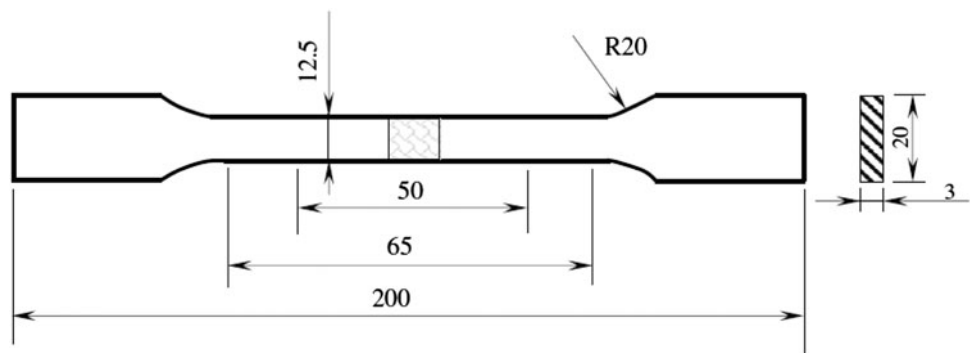
Table 2 Welding parameters of FSW 2014-T6 joints used in this investigation

Sample no.	Rotation speed (rpm)	Welding speed (mm/min)
1	1070	40
2	1070	80
3	1070	112
4	1520	40
5	1520	80
6	1520	112
7	2140	80

Table 1 Chemical composition (wt%) of 2014 aluminum plate used in this investigation

Al	Si	Fe	Cu	Mn	Mg	Zn	Cr	Ni	Ti	Pb
Balance	0.83	0.35	4.16	0.74	0.45	0.10	0.05	0.01	0.02	0.01

zones. Vickers micro-hardness tests were performed along the centerlines of the cross-sections perpendicular to the welding direction using a 300 g load for 15 s. In each testing line the micro-hardness measurements in the weld zone were spaced by intervals of 1 mm. The configuration and size of the transverse tensile specimens were prepared with reference to TS 138 EN 10002-1 [21] (Fig. 2). Tensile tests were carried out on a UTEST-7014 tensile testing machine at room temperature in laboratory air using a constant crosshead speed of 10 mm/min. The property data for each weld were obtained by averaging three test results. The fatigue test specimen design respects the standard requirements. The dimensions of the fatigue test specimens were 25 mm width, 200 mm length and 3 mm thickness. The weld was transverse to the stress axis in the fatigue test specimen (cross-weld). Prior to a fatigue test, the surface of the gauge section was mechanically polished using a water proof silicon abrasive-paper of 1200 grade to prevent fatigue cracking. The fatigue tests have been performed on a uniaxial bending fatigue test machine at a frequency of 20 Hz at room temperature in laboratory air. The fatigue test machine configuration can be seen schematically in Fig. 3. The fatigue tests have been conducted with constant stress amplitude under axial load with $R = \sigma_{min}/\sigma_{max} = -1$ until complete failure occurs.

3 Results and Discussion

3.1 Microstructure

The optical microscopy observations performed on the cross-section of the welded samples revealed the distinct changes in microstructures of the weld zones (Fig. 4). BM microstructure reveals the elongated grains belonging to the rolling operations (Fig. 4a). In the weld centre lies the NZ, which has experienced high temperatures and extensive plastic deformation, and is characterized by dynamically recrystallized grains during FSW process (Fig. 4b, c). Such recrystallized structure is characterized by a very low level of residual stresses, excellent ductility and
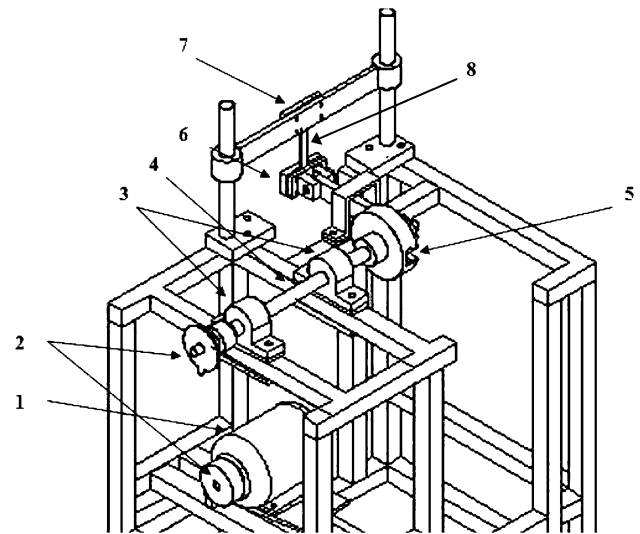

Fig. 3 Scheme of the fatigue test machine (*1* electric motor, *2* belt-pulley mechanism, *3* bearings, *4* main shaft, *5* amplitude control system (flywheel), *6* steering joint, *7* fixed joint, *8* test sample)

mechanical properties superior to those of HAZ [22]. Di et al. [20] reported that these fine-equiaxed recrystallized grains in the NZ could benefit to fatigue performance with longer initiating life of fatigue microcracks and higher fatigue crack growth resistance if fatigue crack was produced in the NZ. On the advancing side (AS), the speed of plastic material is greater than on the retreating side (RS), microstructure changes rapidly, a typically distinct boundary between the NZ and TMAZ (Fig. 4d). This boundary on the AS often has the poor property [3, 14, 23]. On the other side, on the RS, microstructures from the NZ to TMAZ change more smoothly (Fig. 4e). In the TMAZ (Fig. 4f, g), the combination of high stress and large strains causes deformation of grain structure but no recrystallization takes place [5]. In the region adjacent to the TMAZ, i.e. HAZ, the microstructure in the HAZ, which is affected by the heat but not by deformation, is similar to that of BM; the grains are slightly overgrown as a result of the exposure to welding heat. Mahoney et al. [4, 24] defined the HAZ as a zone experiencing a temperature rise above 250°C for a
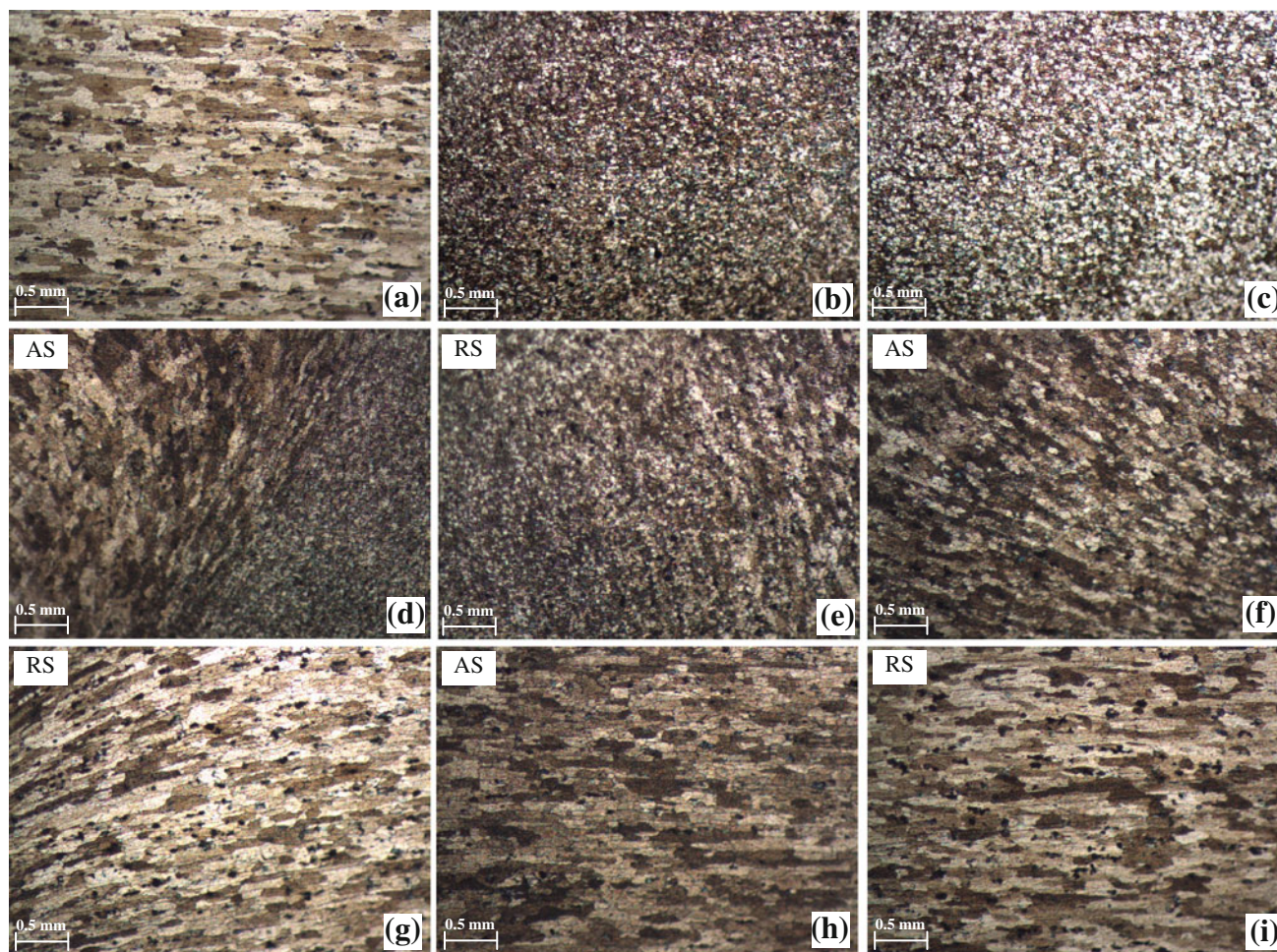
Fig. 4 Microstructures in various zones of FSW 2014-T6 joints: **a** BM; **b**, **c** NZ; **d**, **e** transition zone from NZ to TMAZ; **f**, **g** TMAZ; **h**, **i** HAZ. **b** 1520 rpm–80 mm/min; **c** 1070 rpm–40 mm/min; **d–f**, **h** 1520 rpm–40 mm/min; **g**, **i** 2140 rpm–80 mm/min (*AS* advancing side; *RS* retreating side)

heat-treatable aluminum alloy. However, the thermal exposure above 250°C results in significant coarsening of the precipitates and development of the precipitate free zone (PFZ) [25–28]. From the contrast difference in the grains on the AS and RS, it can be said that the coarsening of the precipitates on the AS is more effective than on the RS due to the high thermal exposure during FSW (Fig. 4d–i).

3.2 Microhardness

The hardness profile of the FSW joints welded with various welding parameters may also be a direct indicator of microstructural evolution during FSW. The hardness profile evolution across the welds is shown in Figs. 5, 6, 7 that a hardness degradation region composed of NZ, two TMAZs and two HAZs has occurred in the joints. However, exception of the joint with a welding speed of 80 mm/min at 1520 rpm the hardness values in the NZs are

lower than in the BM, but higher than in the TMAZ and HAZ. An increase in hardness in the NZs compared to TMAZs and HAZs confirms that some degree of work hardening (intensive stirring) has taken place during FSW process. In addition, some of the precipitates in the NZs might have taken into solution during FSW; it also follows the raise in hardness [29].

A softened region has been formed in the welded region of BM due to frictional heat as it occurs in the joints of the heat treatable aluminium alloys [5]. The hardness profiles of FSW joints in particle-hardened materials are mainly governed by thermal exposure during FSW (viz., by the distribution of the precipitates) [9]. The joints exhibit a hardness drop in around the HAZ and TMAZ indicating that these regions have undergone an overageing/annealling process (dissolution and growth of precipitates). The hardness of the unaffected BM is around 140–150 HV0.3 for the T6 temper condition. Minimum hardness zones with around 110–120 HV0.3 were detected at around HAZ and

Fig. 5 Microhardness profiles of the joints welded at various welding speeds at 1070 rpm (*AS* advancing side; *NZ* Nugget zone; *RS* retreating side)
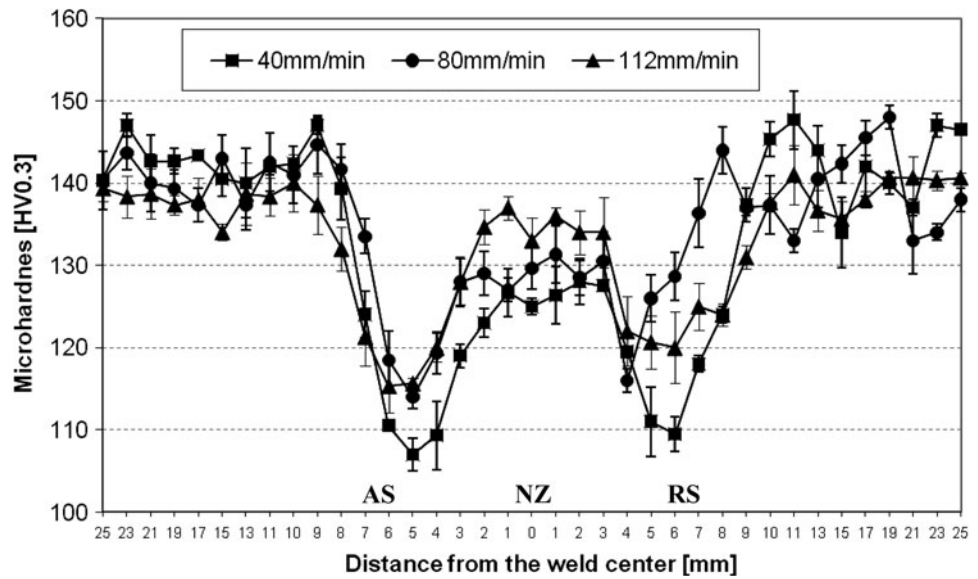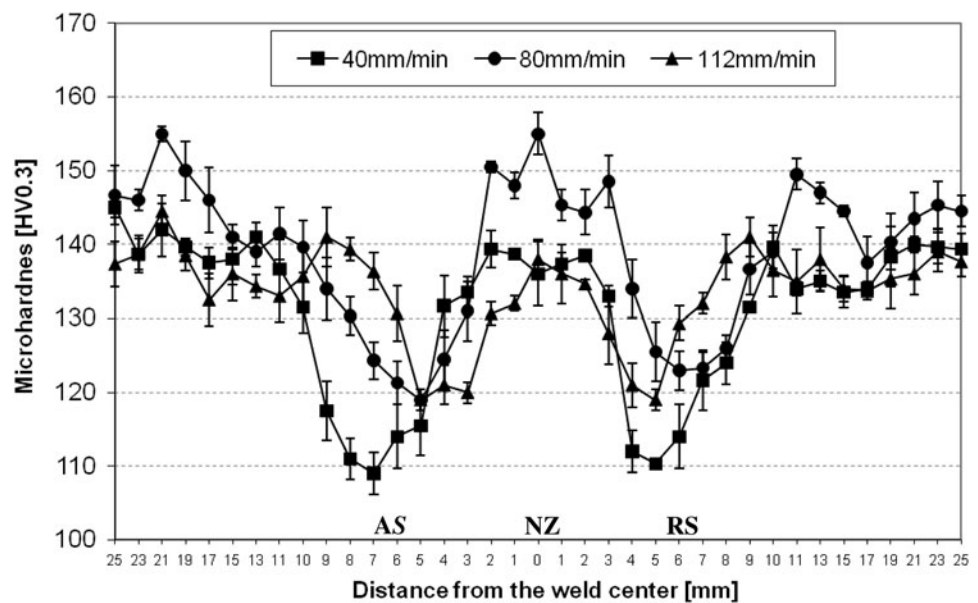

Fig. 6 Microhardness profiles of the joints welded at various welding speeds at 1520 rpm (*AS* advancing side; *NZ* Nugget zone; *RS* retreating side)

TMAZ from the weld centre on both sides of the weld. An average decrease of hardness in these softened regions is around 20%. Rajamanickam et al. [5] reported that the hardness loss in the softened region of the same alloy in the T6 temper state was around 32%. This can be attributed to relatively low welding speeds in their study. In the present study, the hardness loss in the softened region has been reduced with relatively high welding speeds.

The FSW joints welded at the welding speed of 40 mm/min exhibited the lowest hardness values in around the HAZ and TMAZ on both AS and RS indicating that the thermal exposure was higher (Figs. 5, 6). The hardness in the softened region decreases with decreasing the welding speed. The lowest hardness values on the AS of the samples were slightly lower than those on the RS. This is

attributed to a higher temperature on the AS [4]. On the other hand, the hardness values in the softened region slightly increases with increasing the rotating speed under the investigated welding parameters. The width of the softened region is smaller for the low rotating speed specimens, but the maximum depth of the softened region is somewhat larger.

3.3 Tensile Properties

The transverse tensile properties of BM and 2014-T6 FSW joints welded at different welding speeds and rotation speeds are summarized in Table 3. Compared to the BM, generally, the FSW joints exhibited reduced tensile properties, especially ductility, due to the altered and overaged

Fig. 7 Microhardness profiles of the joints welded at various rotating speeds at 80 mm/min (*AS* advancing side; *NZ* Nugget zone; *RS* retreating side)
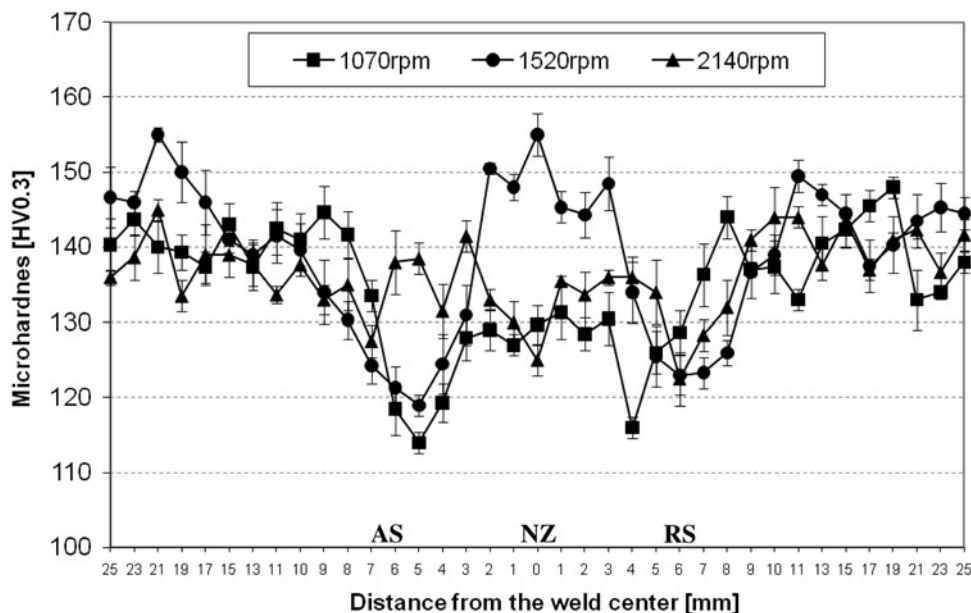

Table 3 Transverse tensile properties and fracture locations of BM and FSW 2014-T6 joints

Rotation speed (rpm)	Welding speed (mm/min)	PHI	APR (mm/r)	YS Rp0.2 (MPa)	UTS Rm (MPa)	Elongation A (%)	Fracture locations of the joints
Base metal		–	–	326 ± 2	452 ± 3	13.0 ± 0.5	–
1070	40	28623	0.0374	303 ± 1	398 ± 1	4.0 ± 0.1	The interface between the NZ and the TMAZ on the AS
1070	80	14311	0.0748	318 ± 2	419 ± 2	5.9 ± 0.2	Around HAZ and TMAZ on the AS
1070	112	10222	0.1047	318 ± 1	393 ± 1	2.9 ± 0.2	Around NZ on the AS
1520	40	57760	0.0263	311 ± 1	404 ± 2	4.4 ± 0.3	The interface between the NZ and the TMAZ on the AS
1520	80	28880	0.0526	343 ± 1	430 ± 3	7.8 ± 0.2	Around HAZ and TMAZ on the AS
1520	112	20629	0.0737	333 ± 2	400 ± 1	2.8 ± 0.1	Around NZ on the AS
2140	80	57245	0.0374	333 ± 2	440 ± 5	6.5 ± 0.2	Around HAZ and TMAZ on the AS

PHI Pseudo Heat Index; *APR* Advance per Revolution; *YS* yield strength; *UTS* ultimate tensile strength

microstructure in the weld zone during FSW process [4, 24].

Mechanical performances of the FSW joints are strongly affected by the heat input. To evaluate heat input during FSW process, heat indexes such as Pseudo Heat Index (PHI) and Advance per Revolution (APR) can be defined in the following equations depending on tool rotation speed (rpm) and welding speed (mm/min) [4]:

$$PHI = \frac{rpm^2}{mm/min} \tag{1}$$

$$APR = \frac{mm/min}{rpm} \tag{2}$$

Friction stir welding joints produced at the same PHI or APR did not exhibit the similar tensile properties (Table 3), indicating that both values may not be used as the

parameters to describe the tensile properties of the FSW 2104-T6 joints under the investigated welding parameters in this study, which is in agreement with the results in FSW age hardenable 6061-T651 aluminum alloy reported by Ren et al. [4]. FSW joints with the same PHI or APR did not also exhibit the same hardness profiles (Figs. 5, 6, 7). These results indicate that a considerable correlation could not be established in between heat indexes and mechanical properties of FSW 2014-T6 joints under the investigated parameters.

The welding parameters exerted noticeable effect on the tensile properties of the FSW joints. Irrespective of the tool rotation speeds, in the tested range the FSW joints with the welding speed of 80 mm/min exhibited the higher tensile properties. For the welding speed of 80 mm/min, the FSW joints exhibited ultimate tensile strength efficiency

(UTS$_{FSW}$/UTS$_{Base}$) of 93–97% and elongation efficiency (E$_{FSW}$/E$_{Base}$) of 45–60%, whereas at the welding speeds of 40 and 112 mm/min, lower tensile strength efficiency of 87–89% and elongation efficiency of 22–34% were observed. The joints welded with a welding speed of 80 mm/min at 1520 rpm showed the best tensile properties (Table 3). On the other hand, welding performances in yield strength of the joints were around that of BM with the exception of the joints with a welding speed of 40 mm/min which have high heat input during FSW.

It is well known that heat input during FSW process plays an important role on the mechanical properties of the joints. Rajamanickam et al. [5] reported that tensile properties of FSW 2014-T6 joints increase with increase in welding speed in the relatively low welding speeds (8, 12 and 20 mm/min). On the other hand, Ericsson and Sandström [10] observed that the welding speed, in much high welding speed range, had no major influence on the tensile properties of FSW 6082 age-hardenable aluminum alloy joints. In the present study, relatively high welding speeds (40, 80 and 112 mm/min) were used. Thermal effect can be seen in the joints produced with the welding speeds of 40 and 80 mm/min. The tensile properties of these joints at the same rotating speed increase with increasing of the welding speed (Fig. 8). This can be attributed to the decreased heat input and relative limited softening of the HAZ and TMAZ

[5]. However, the joints welded at 112 mm/min have lower tensile properties, especially ductility. This could be associated that the stirring effect, material flow and creation of the weld in these joints for heat generation might be presumably less efficient due to the high welding speed. By increasing the welding speed of the tool is extruded too fast and then the joints could not be reached the conditions for the proper mixing and sufficient bonding [10, 30]. Thus, the fractures in the joints welded at 112 mm/min, which have low ductility, occurred in around NZ on the AS, whereas the joints welded at 80 mm/min, which have relatively high ductility, failed at around HAZ and TMAZ on the AS corresponding the softest points of the joints. On the other hand, the fractures in the joints welded at 40 mm/min, which have high heat input during FSW process, occurred in the interface between the NZ and TMAZ on the AS, which is the remarkable difference in the internal structure between the NZ and the TMAZ. All tested tensile specimens failed on the AS of the welds, which is exposed to the highest maximum temperature during FSW. Rajamanickam et al. [5] have also found all tensile fracture occurred in the AS in FSW 2014 joints.

Figure 9 shows the comparison of tensile properties of the joints welded at 80 mm/min in different rotating speeds. When the rotational speed was increased from 1070 to 2140 rpm, correspondingly the strength of weld also
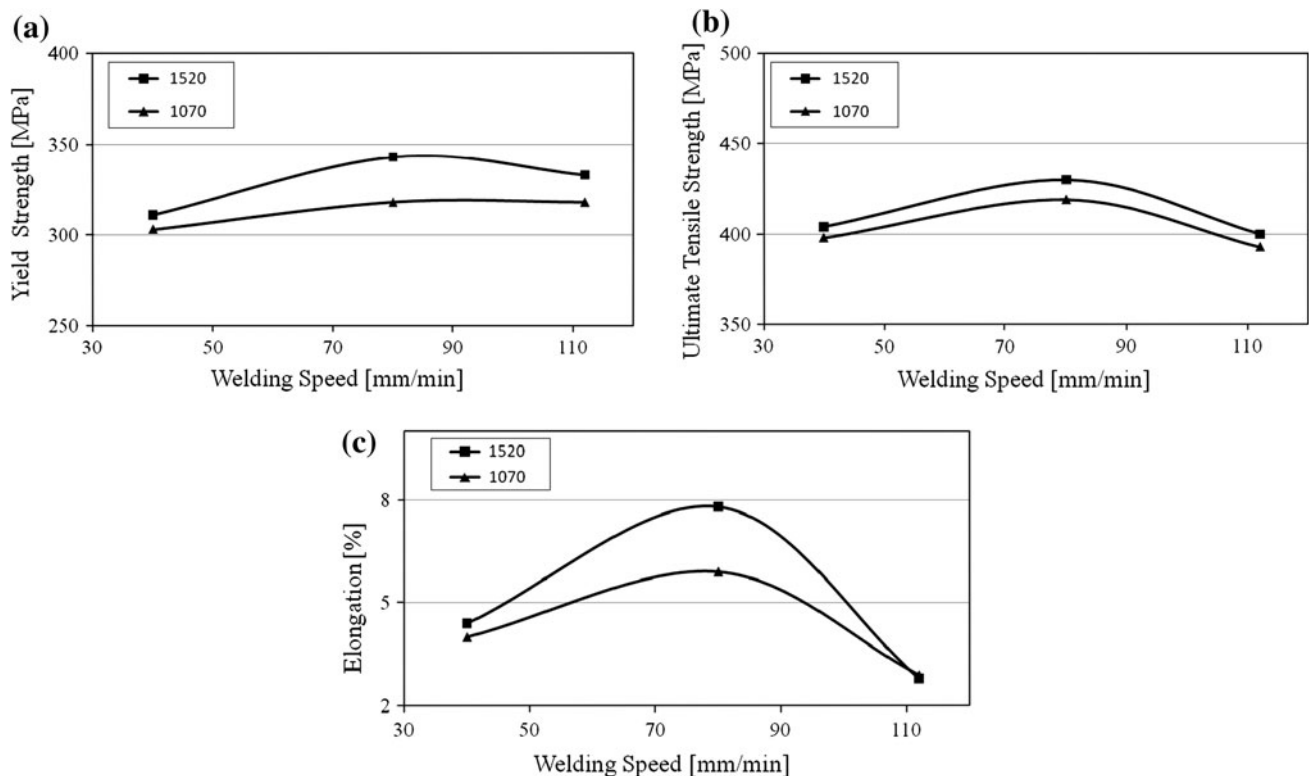

Fig. 8 Comparison of tensile properties of the joints: **a** yield strength; **b** ultimate tensile strength; **c** elongation
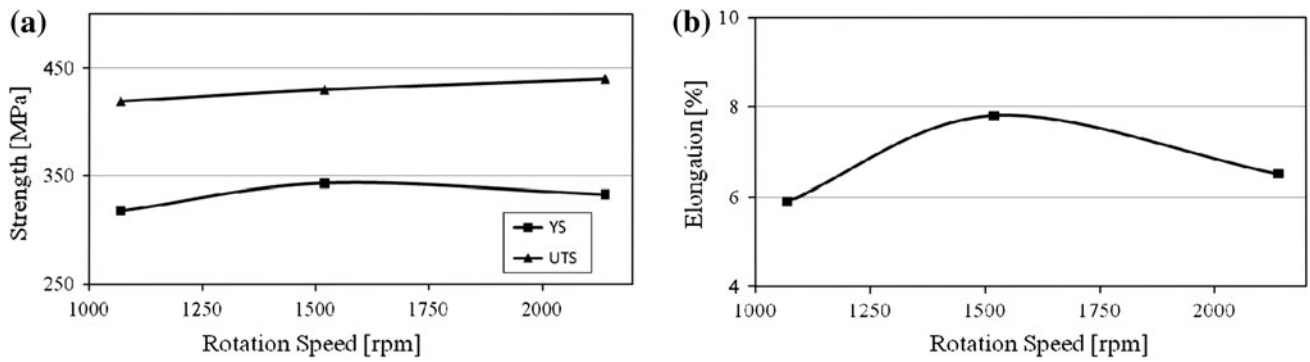
Fig. 9 Comparison of **a** strength and **b** elongation of the joints welded at 80 mm/min
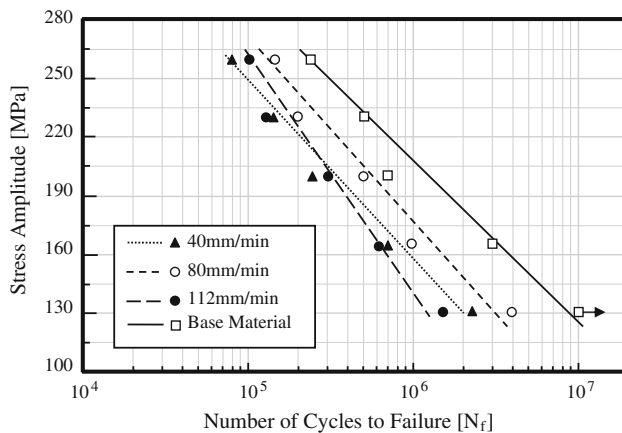

Fig. 10 S–N curves of the FSW joints in different welding speeds at 1070 rpm (the *arrow points* to unbroken specimens)

Fig. 11 S–N curves of the FSW joints in different welding speeds at 1520 rpm (the *arrow points* to unbroken specimens)

slightly increased similarly to the hardness profiles, but the elongation of the weld at 2140 rpm significantly decreased.

3.4 Fatigue Behaviour

The fatigue data of the FSW joints were expressed as stress amplitude versus the corresponding life to failure (i.e. number of cycles) as represented in S–N diagrams (Figs. 10, 11, 12). The fatigue performances of all FSW joints are clearly lower than that of the BM. This result can be connected to the lower ductility of the joints and various microstructure zones in the weld region, which raise the influence of stress concentrations, and so fatigue cracks propagates easily and faster in the weld zone. Cavaliere and Panella [31] have also reported that FSW joints could offer fatigue limits lower than their corresponding base materials, but these limits are extremely higher if compared with those consequent to traditional fusion welds.

There are major differences in fatigue behaviors between the FSW joints in different welding conditions. In the range of the selected welding parameters, the specimens joined with a welding speed of 80 mm/min clearly produce better fatigue endurance for any tool rotation
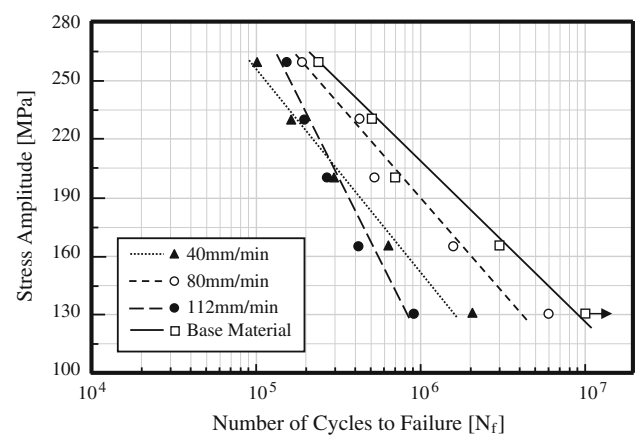
speeds, according to satisfying ductility and strength requirements (Figs. 10, 11, 12). The fatigue life of the joints with a rotating speed of 1520 rpm at 80 mm/min, which show the best fatigue behavior in the FSW joints, reaches 6×10^6 cycles at the stress amplitude of 130 MPa.

In the high stresses, the joints welded with a welding speed of 112 mm/min seems to exhibit higher cycles to failure at the same stress amplitude than the welds joined with a welding speed of 40 mm/min (Figs. 10, 11). On the other hand, in the low stresses, the welds joined with a welding speed of 40 mm/min show the longer fatigue endurance life than the joints welded with a welding speed of 112 mm/min (Figs. 10, 11). In the fatigue tests, 40 mm/min welding speed is more beneficial than the welding speed of 112 mm/min at low stresses. The higher ductility is advantageous for longer fatigue lives at low stresses, since the main part of the fatigue life is related to crack initiation [10]. Figure 12 also shows the influence of rotating speed on the fatigue behaviours of the FSW joints. These results are completely consistent with the elongations of the FSW joints. Higher ductility makes the material less sensitive to stress concentration in the cycling
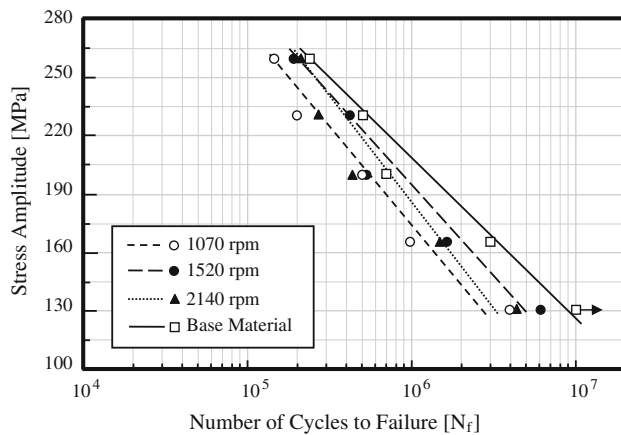
Fig. 12 S–N curves of the FSW joints in different rotation speeds at of 80 mm/min (the *arrow points* to unbroken specimens)

loading. The FSW joints with a rotating speed of 1520 rpm at 80 mm/min, which have highest ductility, show the best fatigue performance, whereas the FSW joints with a rotating speed of 1070 rpm at 80 mm/min, which have lowest ductility, exhibit the lowest fatigue life.

Considering all fatigue results, a significant correlation has not been possible to establish between the welding parameters and fatigue behaviors of the FSW joints. Ericsson and Sandström [10] has not also found a considerable correlation between the welding speed and fatigue behavior of FSW 6082 age-hardenable aluminum joints. However, the fatigue behaviors of all FSW joints are almost consistent with the tensile properties of the joints, especially elongations. In addition, from Figs. 10, 11, 12, it can be said that the welding speed is more effective on the fatigue behaviors of the FSW 2014-T6 joints than the rotation speed.

Almost all FSW joints fatigue loaded failed within the weld zone. High stress fractures of the joints with a welding speed of 80 mm/min often took place in around the NZ and TMAZ on the AS, whereas at low stresses and long lives they appeared in the HAZ, either on the AS or RS, no preference could be seen. In a few cases for the welds with 80 mm/min at 1520 rpm fracture at low stresses was in the BM. Long fatigue lives can be associated with HAZ crack propagation which was a comparatively slower process than the crack propagation in near the NZ and TMAZ. These results are in accordance with the observations made by Ericsson and Sandström [10]. On the other hand, the fractures of the joints with 40 and 112 mm/min took place in near the NZ and TMAZ at all stress levels. When the FSW joints have low ductility, fatigue crack propagates to the NZ/TMAZ boundary on the AS and follows it. This boundary often has the poor mechanical properties due to stress intensity between very fine and coarse grains [3, 14, 23]. However, the fracture locations of these joints become closer to the NZ at higher stress levels. In these joints, the fractures occurred in TMAZ were on the AS or RS, whereas the fractures occurred in the NZ/TMAZ boundary were always on the AS.

4 Conclusions

Tensile properties and fatigue behaviors of 2014-T6 friction stir welded aluminium alloy sheets using different welding parameters have been studied. From this investigation, the following conclusions can be derived:

An average decrease of hardness in the softened weld regions was around 20% under the investigated welding parameters. The hardness in the softened region decreases with decreasing the welding speed. On the other hand, the hardness values in the softened region and the tensile strength of the joints slightly increases with increasing the rotating speed.

Tensile and fatigue properties of the FSW joints are strongly dependent on the welding parameters, especially welding speed. The ductility and strength of the joints reached higher values at welding speed of 80 mm/min under the investigated welding speeds. The joints welded with a welding speed of 80 mm/min at 1520 rpm exhibited the best tensile properties. The fatigue behaviors of the joints are almost consistent with the tensile properties, especially elongations. Higher ductility in FSW joints made the material less sensitive to fatigue. The joints with a welding speed of 80 mm/min had better fatigue performance under the investigated welding parameters. The welds joined with a welding speed of 80 mm/min at 1520 rpm showed the best fatigue behavior.

The location of tensile fractures of the joints is dependent on welding parameters. In the joints welded at 80 mm/min, which have high ductility, the tensile fractures occurred in around the HAZ and TMAZ on the AS, whereas the joints welded at 112 mm/min, which have low ductility, failed in around the NZ on the AS. On the other hand, the fractures in the joints welded at 40 mm/min, which have high heat input during FSW, occurred in the interface between the NZ and TMAZ on the AS.

The fatigue fracture locations change depending on the welding parameters and stress range. High stress fatigue fractures of the joints with a welding speed of 80 mm/min took place in around the NZ and TMAZ on the AS, whereas at low stresses and long lives they appeared in the HAZ, either on the AS or RS. On the other hand, the fatigue fractures of the joints at 40 and 112 mm/min occurred in around the NZ and TMAZ at all stress levels. However, the fracture locations of these joints become closer to the NZ at higher stress levels.

A considerable correlation could not be established in between heat indexes and mechanical properties of FSW 2014-T6 joints under the investigated welding parameters.

References

1. Thomas W M, Nicholas E D, Needham J C, Church M G, Temple-Smith P, and Dawes C J, GB Patent Application, No. 9125978-9 (1991).
2. Mishra R S, Ma Z Y, and Charit I, *Mater Sci Eng A* **341** (2003) 307.
3. Zhao Y h, Lin S b, Wu L, and Qu F x, *Mater Lett* **59** (2005) 2948.
4. Ren S R, Ma Z Y, and Chen L Q, *Scr Mater* **56** (2007) 69.
5. Rajamanickam N, and Balusamy V, *Indian J Eng Mater Sci* **15** (2008) 293.
6. Vural M, Ogur A, Cam G, and Ozarpa C, *Arch Mater Sci Eng* **28** (2007) 49.
7. Lockwood W D, Tomaz B, and Reynolds A P, *Mater Sci Eng A* **323** (2002) 348.
8. Dawes C J, in *Friction Stir Welding, in Training in Aluminium*, Application Technologies-TALAT, European Aluminum Association, in CD-ROM Lectures 4410 (1990).
9. Babu G R, Murti K G K, and Janardhana G R, *ARPN J Eng Appl Sci* **3** (2008) 68.
10. Ericsson M, and Sandström R, *Int J Fatigue* **25** (2003) 1379.
11. Dickerson T, Shi Q, and Shercliff H R, in 4th Int. Symposium on Friction Stir Welding *Heat Flow into Friction Stir Welding Tools,*, Park City, UT, USA (2003).
12. Jata K V, and Semiatin S L, *Scr Mater* **43** (2000) 743.
13. Salem H G, Reynolds A P, and Lyons J S, *Scr Mater* **46** (2002) 337.
14. Aydin H, Bayram A, Uğuz A, and Akay S K, *Mater Des* **30** (2009) 2211.
15. Uematsu Y, Tokaji K, Shibata H, Tozaki Y, and Ohmune T, *Int J Fatigue* **31** (2009) 1443.
16. Aydin H, Bayram A, Yıldırım M T, and Yiğit K, *Mater Sci Medziagotyra* **16** (2010) 311.
17. Zhou C, Yang X, and Luan G, *Scr Mater* **53** (2005) 1187.
18. Lomolino S, Tovo R, and dos Santos J, *Int J Fatigue* **27** (2005) 305.
19. Dickerson T L, and Przydatek J, *Int J Fatigue* **25** (2003) 1399.
20. Di S, Yang X, Luan G, and Jian B, *Mater Sci Eng A* **435–436** (2006) 389.
21. Turkish Standard, TS 138 EN 10002-1, *Metallic Materials—Tensile Testing—Part 1: Method of Test at Ambient Temperature*, Turkey (2004).
22. Salem H G, *Scr Mater* **49** (2003) 1103.
23. Aydin H, Bayram A, and Durgun I, *Mater Des* **31** (2010) 2568.
24. Mahoney M W, Rhodes C G, Flintoff J G, Bingel W H, and Spurling R A, *Metall Mater Trans A* **29** (1998) 1955.
25. Mishra R S, and Ma Z Y, *Mater Sci Eng R* **50** (2005) 1.
26. Sato Y S, Kokawa H, Enomote M, and Jogan S, *Metall Mater Trans A* **30A** (1999) 2429.
27. Benavides S, Li Y, Murr L E, Brown D, and McClure J C, *Scr Mater* **41** (1999) 809.
28. Jata K V, Sankaran K K, and Ruschau J, *Metall Mater Trans A* **31** (2000) 2181.
29. Denquin A, Allehaux D, Campagnac M–H, and Lapasset G, in Proceedings of The Third International Symposium on Friction Stir Welding, *Microstructural Evolution and Strength Mismatch Within a Friction Stir Welded 6056 Aluminium Alloy*, Kobe, Japan (2001).
30. Cavalierea P, Squillace A, and Panella F, *J Mater Process Technol* **180** (2008) 364.
31. Cavaliere P, and Panella F, *J Mater Process Technol* **206** (2008) 249.